

Title page and abstract

1 **Segment 2 from influenza A(H1N1)pdm09**
2 **viruses confers temperature sensitive HA yield**
3 **on candidate vaccine virus growth in eggs that is**
4 **complemented by PB2 701D**

5
6 **Saira Hussain^{1,2}, Matthew L. Turnbull^{1#}, Rute M. Pinto^{1#}, John W. McCauley²,**
7 **Othmar G. Engelhardt³ & Paul Digard^{1*}**

8
9 ¹The Roslin Institute & Royal (Dick) School of Veterinary Studies, University of
10 Edinburgh, EH25 9RG, United Kingdom; ²The Francis Crick Institute, London, NW1
11 1AT, United Kingdom; ³National Institute for Biological Standards and Control,
12 Hertfordshire, EN6 3QG, United Kingdom.

13
14 [#]Present address: Glasgow Centre for Virus Research, Glasgow, G61 1QH, United
15 Kingdom

16
17 *Corresponding author: Professor Paul Digard

18 Tel: +44 131 651 9240

19 Email: paul.digard@roslin.ed.ac.uk

20
21 Main text word count: 5265

22 Abstract word count: 248

Title page and abstract

23 **Abstract**

24

25 Candidate vaccine viruses (CVVs) for seasonal influenza A virus are made by
26 reassortment of the antigenic virus with a high-yielding egg-adapted strain, typically
27 A/Puerto Rico/8/34 (PR8). Many 2009 H1N1 pandemic (pdm09) high-growth
28 reassortants (HGRs) selected by this process contain pdm09 segment 2 in addition to the
29 antigenic genes. To investigate this, we made CVV mimics by reverse genetics (RG) that
30 were either 6:2 or 5:3 reassortants between PR8 and two pdm09 strains,
31 A/California/7/2009 (Cal7) and A/England/195/2009, differing in the source of segment
32 2. The 5:3 viruses replicated better in MDCK-SIAT1 cells than the 6:2 viruses, but the
33 6:2 CVVs gave higher HA antigen yields from eggs. This unexpected phenomenon
34 reflected temperature sensitivity conferred by pdm09 segment 2, as HA yields from eggs
35 for the 5:3 viruses improved substantially when viruses were grown at 35°C compared
36 with 37.5°C, whereas 6:2 virus yield did not. Authentic 5:3 pdm09 HGRs, X-179A and
37 X-181, were not markedly temperature-sensitive however, despite their PB1 sequences
38 being identical to that of Cal7, suggestive of compensatory mutations elsewhere in the
39 genome. Sequence comparisons of the PR8-derived backbone genes identified single
40 changes in PB2 and NP, 5 in NS1, and 1 in NS2. PB2 N701D but not NP T130A affected
41 the temperature dependency of viral transcription. Furthermore, introducing the PB2
42 701D change into a 5:3 CVV mimic improved and drastically reduced the temperature
43 sensitivity of HA yield. We conclude that RG PR8 backbones used for vaccine
44 manufacture in eggs should contain PB2 701D to maximise virus yield.

45

46 **Keywords:** influenza, vaccine, PB1, PB2, temperature sensitive

Introduction

47 **Introduction**

48

49 Worldwide, annual influenza epidemics result in three to five million cases of
50 severe illness, and 250,000 to 500,000 deaths [1]. Both influenza A viruses (IAV) and
51 influenza B viruses cause seasonal disease but IAV poses additional risks of sporadic
52 zoonotic infections and novel pandemic strains. IAVs are divided into subtypes by
53 their antigenic determinants, the surface glycoproteins haemagglutinin (HA) and
54 neuraminidase (NA). Pandemics have occurred with H1N1 (in 1918 and 2009), H2N2
55 (1957) and H3N2 (1968) subtype viruses; currently circulating epidemic viruses
56 descended from these are from the H3N2 and 2009 H1N1 (pdm09) lineages.

57 The primary measure to control influenza is vaccination. Seasonal vaccine
58 production techniques rely on classical reassortment to generate viruses with good
59 growth properties in embryonated hens' eggs, the major manufacturing substrate. This
60 involves co-infecting eggs with the antigenic (vaccine strain) virus of choice along
61 with a high yielding ("donor") virus already adapted to growth in eggs. Reassortant
62 viruses that contain the HA and NA of the vaccine viruses are selected and the highest
63 yielding viruses, (high growth reassortants or HGRs), are designated as candidate
64 vaccine viruses (CVVs). Generating HGRs with the desired growth properties can be
65 difficult and sometimes requires further passaging of the initial reassortants to further
66 adapt them to growth in eggs, which can also induce unwanted antigenic changes to
67 the HA [2-7].

68 An alternative, potentially quicker method to generate HGRs that,
69 conceptually at least, reduces potential antigenic changes, involves using reverse
70 genetics (RG) to create the desired strain [8-10]. This method involves generation of
71 virus by transfection of cells with plasmids encoding the eight genomic segments of

Introduction

72 IAV which transcribe both viral mRNA and negative sense viral RNA (vRNA),
73 resulting in the *de novo* production of virus particles. Typically, the six viral backbone
74 segments (segments 1, 2, 3, 5, 7 and 8) are derived from the egg-adapted donor strain,
75 whereas the two segments encoding HA and NA are derived from the vaccine strain.
76 This “6:2” reassortant can then be produced in large scale in eggs. RG is the only
77 currently viable method to produce CVVs for highly pathogenic avian IAV strains,
78 since it allows the deletion of polybasic sequences that are determinants for high
79 pathogenicity from the virus HA.

80 A limited number of donor strains for IAV vaccine manufacture exist. The
81 strain that underpins both classical reassortment and RG approaches is the A/Puerto
82 Rico/8/34 strain (PR8). However, reassortant IAVs with PR8 backbone segments do
83 not always grow sufficiently well to ensure efficient vaccine manufacture, prompting
84 the need for better understanding of the molecular determinants of CVV fitness.
85 Analysis of conventionally derived HGR viruses has shown that as expected, PR8-
86 derived internal segments predominate, with 6:2 and 5:3 (PR8:WT virus) reassortants
87 representing the most common gene constellations. Of the 5:3 HGRs, segment 2 is the
88 most common third vaccine virus-derived segment, especially in human pdm09, but
89 also in H3N2 and H2N2 subtypes [11, 12]. In addition, an avian H5N2 5:3
90 reassortant was shown to produce higher yields than its 6:2 counterpart [13]. Since all
91 6 internal PR8 gene segments are presumably adapted to growth in eggs, this
92 preference for the vaccine strain PB1 gene perhaps indicates that it confers a growth
93 advantage in the presence of the vaccine strain HA and/or NA genes. Supporting this,
94 many studies have used RG to confirm that introducing a vaccine virus-derived
95 segment 2 into CVV mimics can improve virus yield for human pdm09 and H3N2
96 strains, as well as avian H5N1 and H7N9 strains [14-22]. Moreover, it has been

Introduction

97 shown that CVV 5:3 reassortants containing a pdm09 segment 2 and glycoproteins of
98 avian H5N1 and H7N9 viruses also give higher yields than their respective 5:3 viruses
99 containing the indigenous WT segment 2, suggesting a particular growth advantage
100 conferred to CVVs by the pdm09 segment 2 [22].

101 The fitness advantage conferred by WT segment 2 may be at the genome
102 packaging level [17, 23, 24], and/or due to a positive contribution from the coding
103 region of segment 2. Segment packaging signals of the glycoprotein genes are known
104 to influence yield [14, 25-32] and it has been demonstrated for H3N2 subtype 5:3
105 reassortants that the NA and PB1 segments co-segregate, driven by interactions in the
106 coding region of segment 2 [17, 22]. However, this does not exclude contributions
107 from the encoded proteins, complicated by the fact that segment 2 produces at least
108 three polypeptide species: the viral polymerase PB1, a truncated version of PB1, PB1-
109 N40, and from an overlapping reading frame, a virulence factor PB1-F2 [33-35].
110 Moreover, various PR8 strains are used to make HGRs which can give rise to
111 different growth phenotypes for CVVs containing glycoprotein genes from the same
112 strain/subtype [13, 36]. Overall therefore, a better understanding of the molecular
113 basis for the effects of vaccine strain-derived segment 2s on growth of reassortant
114 IAVs in eggs is needed, to better enable rational design of CVVs.

115 As a starting point, we rescued CVV mimics that were either 6:2 or 5:3
116 reassortants between PR8 and pdm09 viruses that differed in whether they contained
117 pdm09 or PR8 segment 2. The expectation, based on empirical evidence and previous
118 studies was that the 5:3 reassortants would grow better than the 6:2 ones. This turned
119 out not to be the case; a result that ultimately led to the identification of PB2 residue
120 701D as crucial for facilitating the HGR-enhancing characteristics of pdm09 segment
121 2 in eggs.

Methods

122 **Materials and methods**

123

124 **Cell lines and viruses**

125 Human embryonic kidney (293T) cells, Madin-Darby canine kidney epithelial
126 cells (MDCK) and MDCK-SIAT1 (stably transfected with the cDNA of human 2,6-
127 sialtransferase; [37]) cells were obtained from the Crick Worldwide Influenza Centre,
128 The Francis Crick Institute, London. QT-35 (Japanese quail fibrosarcoma; [38]) cells
129 were obtained from Dr Laurence Tiley, University of Cambridge. Cells were cultured
130 in DMEM (Sigma) containing 10% (v/v) FBS, 100 U/mL penicillin/streptomycin and
131 100 U/mL GlutaMAX with 1 mg/ml Geneticin as a selection marker for the SIAT
132 cells. IAV infection was carried out in serum-free DMEM containing 100 U/mL
133 penicillin/streptomycin, 100 U/mL GlutaMAX and 0.14% (w/v) BSA. All viruses
134 used in this study were made by RG using previously described plasmids for the PR8
135 [39], and A(H1N1)pdm2009 strains A/England/195/2009 (Eng195) [40] and
136 A/California/07/2009 (Cal7) [41]. CVV strains NYMC X-179A (X-179A) and
137 NYMC X-181 (X-181) were obtained from the National Institute for Biological
138 Standards and Control (NIBSC) repository. Virus sequence analyses were performed
139 in part using data obtained from the NIAID Influenza Research Database (IRD) [42]
140 through the web site at <http://www.fludb.org>

141

142 **Antisera**

143 Commercially obtained primary antibodies used were: rabbit polyclonal anti-
144 swine H1 HA (Ab91641, AbCam) and mouse monoclonal anti-NP (Ab128193,
145 AbCam). Laboratory-made rabbit polyclonal anti-NP (2915), anti-M1 (2917) and anti-
146 PB2 have already been described [43-45]. Secondary antibodies used for western blot

Methods

147 were donkey anti-rabbit DyLight 800 and goat anti-mouse DyLight 680-conjugated
148 (Licor Biosciences). Secondary antibodies used for staining plaque or TCID₅₀ assays
149 were goat anti-mouse horseradish peroxidase and goat anti-rabbit horseradish
150 peroxidase (Biorad).

151

152 **Site-directed mutagenesis**

153 The QuikChange® Lightning site-directed mutagenesis kit (Stratagene) was
154 used for mutagenesis according to the manufacturer's instructions. Primers used for
155 site-directed mutagenesis were designed using the primer design tool from Agilent
156 technologies.

157

158 **Reverse genetics rescue of viruses**

159 293T cells were transfected with eight pHW2000 plasmids each encoding one
160 of the IAV segments using Lipofectamine 2000 (Invitrogen). Cells were incubated at
161 37°C, 5% CO₂ for 6 hours post-transfection before medium was replaced with serum-
162 free virus growth medium. At 2 days post-transfection, 0.5 µg/ml TPKC trypsin was
163 added to cells. Cell culture supernatants were harvested at 3 days post-transfection,
164 clarified and used to infect 10-11 day-old embryonated hens' eggs (Henry Stewart
165 Ltd). Following incubation for 3 days at 37.5°C, eggs were chilled overnight and virus
166 stocks were harvested, titred and partially sequenced to confirm identity.

167

168 **RNA extraction, RT-PCR and sequence analysis**

169 Viral RNA extractions were performed using the QIAamp viral RNA mini kit
170 (QIAGEN) using on-column DNase digestion (QIAGEN). Reverse transcription was
171 performed with the Uni12 primer (AGCAAAAGCAGG) using the Verso® cDNA kit

Methods

172 (Thermo Scientific). PCR reactions were performed using Pfu Ultra II fusion 145 HS
173 polymerase (Stratagene) or Taq Polymerase (Invitrogen) according to the
174 manufacturer's protocol. PCR products were purified for sequencing by Illustra GFX
175 PCR DNA and Gel Band Purification kit (GE Healthcare). Primers and purified DNA
176 were sent to GATC biotech (Lightrun method) for sequencing. Sequences were
177 analysed using the DNASTAR software.

178

179 **Virus titration**

180 Plaque assays, TCID₅₀ assays and HA assays were performed according to
181 standard methods [46]. MDCK or MDCK-SIAT cells were used and infectious foci
182 were visualised by either toluidine blue staining or immunostaining for IAV NP and a
183 tetra-methyl benzidine (TMB) substrate. HA assays were performed in microtitre
184 plates using 1% chicken red blood cells/PBS (TCS Biosciences) and all titres are
185 given per 50 µl.

186

187 **Virus purification and analysis**

188 Allantoic fluid was clarified by centrifugation twice at 6,500 x g for 10 mins.
189 Virus was then partially purified by ultracentrifugation at 128,000 x g for 1.5 hours at
190 4°C through a 30% sucrose cushion. Pellets were resuspended in PBS and in some
191 cases treated with N-glycosidase F (PNGase F; New England Biolabs), according to
192 the manufacturer's protocol. Virus pellets were lysed in Laemmli's sample buffer and
193 separated by SDS-PAGE on 10% or 12% polyacrylamide gels under reducing
194 conditions. Protein bands were visualised by Coomassie blue staining (Imperial
195 protein stain, Thermo Scientific) or detected by immunostaining in western blot.
196 Coomassie stained gels were scanned and bands quantified using ImageJ software.

Methods

197 Western blots were scanned on a Li-Cor Odyssey Infrared Imaging system v1.2 after
198 staining with the appropriate antibodies and bands were quantified using ImageStudio
199 Lite software (Odyssey).

200

201 **Quantitative Real-time PCR**

202 RNA extracted from virus pellets (containing partially purified virus from
203 allantoic fluid pooled from two independent experiments) was reverse transcribed
204 (RT) using the Uni12 primer with the Verso® cDNA kit (Life Technologies),
205 according to the manufacturer's instructions. qPCR was based on TaqMan chemistry,
206 primers and probes were designed using the Primer express software version 3.0.1
207 (Applied Biosystems) for Cal7 segments 2 and 6 and PR8 segments 2, 5 and 7. To
208 amplify Cal7 segment 4, Taqman primers/probes were ordered using sequences from
209 the CDC protocol [47]. Due to nucleotide variations between Cal7 and PR8 segment
210 2, different primers/probe were used to amplify the genes from the two strains. Primer
211 and probe sequences are provided in Table 1. PCR was performed using the Taqman
212 Universal PCR Master Mix (Applied Biosystems), according to the manufacturer's
213 instructions with the recommended cycling conditions. Samples were run on a
214 QuantStudio 12k Flex machine (Applied Biosystems) and analysed using the
215 QuantStudio 12k Flex software, applying automatic thresholds. Standard curves were
216 generated using serially diluted linearised plasmid containing cDNA of the matching
217 genes or RT products from viruses of known titre. PCR products from both linearised
218 plasmid templates and RT templates were separated on 3% agarose gels, and
219 fragments of the correct size were distinguished. DNA was excised from the gels and
220 extracted using the Illustra GFX PCR DNA and Gel Band Purification Kit (GE
221 Healthcare), according to the manufacturer's instructions. PCR products were

Methods

222 sequence confirmed by Sanger sequencing where sufficient material for sequencing
223 was obtained. qRT-PCR was performed in triplicate per sample and mock-infected-
224 cell, no-RT (with template) and no-template controls both from the RT reaction and
225 for the qRT-PCR mix only were used in each experiment, always giving
226 undetermined C_T values for the controls. Relative RT levels were calculated by using
227 C_T values for segments from virus pellets from viruses grown at the different
228 temperatures and interpolating from standard curves of RT products of RG 5:3 WT
229 virus grown at 37.5°C for Cal7 segments 2, 4, 6 and PR8 5 and 7 and for PR8
230 segment 2 from the standard curve of RG 6:2 WT virus grown at 37.5°C.

231

232 **Influenza ribonucleoprotein (RNP) reconstitution assays**

233 QT-35 cells at 90% confluency were co-transfected with a chicken pol I firefly
234 luciferase reporter plasmid flanked with segment 8 untranslated regions (UTRs), [48]
235 and four pHW2000 plasmids expressing each of the viral protein components needed
236 to reconstitute RNP complexes using Lipofectamine 2000 (Invitrogen). Triplicate
237 repeats of each assay were performed in parallel at 37.5°C and 35°C. At 48 hours
238 post-transfection, the cells were lysed using Reporter Lysis Buffer (Promega) and
239 luciferase activity measured using Beetle Luciferin (Promega), reconstituted in H₂O
240 and diluted to a final concentration of 0.6mM. Luciferase activity of each
241 reconstituted RNP was normalised to a ‘No PB2’ negative control.

242

243 **Graphs and statistical analyses**

244 All graphs were plotted in and statistical analyses (Tukey’s tests as part of one-
245 way ANOVA) were performed using Graphpad Prism software.

Results

246 Results

247

248 Incorporating a pdm09 segment 2 into CVVs confers temperature sensitivity

249

250 As a starting point, we used RG to rescue candidate vaccine virus (CVV)
251 mimics that were either 6:2 or 5:3 reassortants between PR8 and the early pdm09
252 virus isolates Cal7 and Eng195 that differed in whether they contained a pdm09 or
253 PR8 segment 2 in addition to the pdm09 glycoprotein genes. As comparators,
254 parental (non-reassortant) PR8, Cal7 and Eng195 viruses were also rescued. The
255 expectation, based on empirical evidence from existing HGRs as well as from
256 published work that used RG methods [14-22], was that the 5:3 reassortants would
257 grow better than the 6:2 viruses. Viruses were generated by transfecting 293T cells
258 with the desired plasmids, and amplifying virus in eggs. To assess viral growth,
259 TCID₅₀ titres were determined on MDCK-SIAT cells. The infectious titre of
260 independently rescued stocks of the 5:3 reassortants were on average ~ 2-fold higher
261 than the parental pdm09 viruses and ~ 7-fold higher than the 6:2 reassortants, but
262 around 2 log₁₀ lower than WT PR8 (Figure 1A). Surprisingly however, when the HA
263 titres of virus stocks were measured, the PR8/pdm09 6:2 viruses gave on average ~
264 3-fold higher HA titres than the 5:3 viruses (Figure 1B). When HA:infectivity ratios
265 were calculated, the RG 6:2 viruses showed on average ~ 30-fold higher values than
266 the RG 5:3 viruses (Figure 1C), suggesting an influence of the pdm09 segment 2 on
267 HA content and/or virus particle infectivity.

268 To further assess the effect of the pdm09 segment 2 on virus yield, eggs were
269 inoculated with a dose range from 10 – 1000 TCID₅₀ of virus per egg of the
270 PR8:pdm09 reassortant viruses and allantoic fluid titre measured by HA assay

Results

271 following incubation at 37.5°C for 3 days. The yield of each virus was insensitive to
272 input dose, with no significant differences between average titres within each group
273 of viruses (Figures 2A, B). However, at all doses, the RG Cal7 and Eng195 6:2
274 reassortants gave higher average HA titres than their 5:3 counterparts, and these
275 differences were mostly statistically significant. As before (Figure 1), this was the
276 opposite of the anticipated result, based on the known compositions of
277 conventionally selected pdm09-based CVVs [11]. However, influenza vaccine
278 manufacture often involves incubation of the eggs at temperatures below 37.5°C
279 [49], so we therefore tested the outcome of growing the reassortant viruses in eggs
280 incubated at 35°C. Again, average HA titres were insensitive to inoculum dose, but
281 the differences between the 5:3 and 6:2 pairs were much reduced and no longer
282 statistically significant. (Figures 2C, D). Growth of both the 6:2 and 5:3 PR8:Cal7
283 reassortants was improved at 35°C compared to 37.5°C, by around 2-4 fold for the
284 6:2 virus but by 8-16 fold for the 5:3 virus (Figures 2A, C). Yield of the 6:2
285 PR8:Eng195 virus was not increased by growth at the lower temperature but
286 substantial gains of around 4-fold were seen with the 5:3 reassortant (Figures 2B, D).
287 Thus the 5:3 viruses including a pdm09 segment 2 appeared to be more temperature
288 sensitive than the RG 6:2 viruses.

289

290 **RG 5:3 and 6:2 reassortants differ in their incorporation of HA into virions at** 291 **different temperatures**

292

293 To directly assess HA protein yield, viruses from each experiment were
294 partially purified from equal volumes of pooled allantoic fluid by pelleting through
295 30% sucrose cushions. HA₁ content from virus pellets was analysed by SDS-PAGE

Results

296 and western blotting either before or after treatment with PNGaseF to remove
297 glycosylation. This gave the expected alternating pattern of slow and faster-migrating
298 HA polypeptide species (Figure 3A, top row). The amount of HA₁ fluctuated between
299 samples but for both Cal7 and Eng195 reassortants, yield was generally higher from
300 viruses grown at 35°C than 37.5°C and highest from the 6:2 reassortants. To test the
301 reproducibility of this, de-glycosylated HA₁ was quantified from the western blots of
302 replicate experiments. Absolute HA₁ yield was variable, but across a total of 5
303 independent experiments with 4 technical replicates, the average HA₁ recovery from
304 both PR8:Cal7 and PR8:Eng195 5:3 and 6:2 viruses was improved by growth at 35°C,
305 but by a greater factor (nearly 5-fold versus 3-fold) for the 5:3 reassortants (Figure
306 3B).

307 To test to what extent the varying HA1 yields reflected difference in virus
308 growth and/or HA content of the virus particles, we investigated virion composition
309 by determining the relative amounts of HA₁ to the other two major structural
310 polypeptides, NP and M1. Western blotting showed reasonably consistent amounts of
311 the latter two proteins in the PR8:Cal7 preparations (Figure 3A, left hand side), but
312 more variable and generally lower recovery of NP in the PR8:Eng195 viruses,
313 especially for the 6:2 virus at 37.5°C (right hand panels). Quantification of these
314 proteins from four independent experiments with the PR8:Cal7 viruses (where the
315 higher growth of the viruses allowed more reliable measurements) showed that the
316 NP:M1 ratios were reasonably consistent and not obviously affected by the incubation
317 temperature of the eggs or the source of segment 2 (Figure 3C). However, the RG 5:3
318 virus showed a significantly higher NP:HA₁ ratio than the 6:2 virus when grown at
319 37.5°C but not at 35°C (Figure 3D). Therefore, the inclusion of the pdm09-derived

Results

320 segment 2 into the PR8 reassortants led to exacerbated temperature sensitivity and
321 lower HA content in virus particles.

322

323 **The Cal7 segment 2 does not confer temperature sensitivity to HGRs X-179A**
324 **and X-181**

325

326 Following the observation of temperature sensitivity of our RG 5:3 viruses, we
327 tested whether growth of the RG WT pdm09 viruses and corresponding conventional
328 HGR viruses were similarly affected by temperature. Viruses were grown in eggs at
329 35°C or 37.5°C and the resulting HA titres plotted as fold increases in growth at the
330 lower temperature. Titres of RG viruses containing a PR8 segment 2 were only
331 modestly (~ 2-4 fold) affected by temperature, but those of viruses containing a
332 pdm09 segment 2 were ~ 8-16-fold higher at 35°C than 37.5°C (Figure 4; compare
333 solid blue and red bars). However, the yield of the conventionally reassorted authentic
334 5:3 HGRs X-179A and X-181 (both containing a segment 2 from Cal7 and five other
335 internal gene segments from PR8) were only ~3-4 fold higher at the lower
336 temperature. Thus, the Cal7 segment 2 gene behaved differently in conventional and
337 RG reassortant virus settings; presumably because of sequence polymorphisms in
338 either segment 2 itself and/or the PR8 backbone between what should be, at first sight,
339 equivalent viruses.

Results

340 **Internal segments of RG PR8 and HGR X-179A differ**

341

342 To understand the molecular basis of the temperature sensitivity conferred by
343 RG derived pdm09 segment 2 compared to authentic HGRs, amino-acid sequence
344 comparisons were made between the pdm09-derived genes of the RG viruses used in
345 this study versus those of the HGRs X-179A and X-181. The NA sequences of all
346 four viruses, RG Cal7, RG Eng195, X-179A and X181, were identical (Table 2A).
347 The HA polypeptides of the Cal7, X-179A and X-181 viruses were very similar,
348 differing only with a T209K in the Cal7 sequence and a N129D substitution in the X-
349 181 sequence, while the Eng195 HA varied at four positions from all of the other
350 three viruses and also differed from the HGR viruses in T209K. Within segment 2, the
351 apparent source of the temperature sensitivity, only RG Eng195 differed from the
352 other isolates, with a single amino acid change (R353K). There were no changes in
353 the truncated 11 codon PB1-F2 gene for any of the viruses. Therefore, given the lack
354 of any consistent differences between the two RG pdm09 clones and the conventional
355 HGR viruses, the generally poor and highly temperature sensitive HA yield of the RG
356 5:3 viruses seemed unlikely to be due to segment 2. Instead, we hypothesised that it
357 was due to epistatic effects arising from sequence differences in the PR8 internal
358 segments of the viruses. Comparison of the internal gene sequences of our RG PR8
359 and X-179A (no comparable sequences were available for X-181) showed no coding
360 differences in segments 3 and 7, but several in segment 8 (five in NS1 and one in
361 NS2) and one each in PB2 and NP (Table 2B). Amongst these changes, the PB2
362 N701D polymorphism has been previously linked with host-adaptive changes
363 including temperature sensitivity by several studies [50-58]. Furthermore, PB2
364 N701D is phenotypically linked with the dominant PB2 host-adaptive polymorphism

Results

365 E627K which also affects temperature sensitive viral polymerase activity [59-61].

366 This therefore suggested the hypothesis that the PR8 PB2 contributed to the

367 temperature sensitive phenotype seen here.

368 To test if the temperature sensitivity conferred by segment 2 of pdm09 viruses

369 could be attributed to effects on viral polymerase activity, we performed RNP

370 reconstitution assays using the readily-transfectable avian QT-35 Japanese quail

371 fibrosarcoma cell line at both 37.5°C and 35°C. Cells were transfected with plasmids to

372 reconstitute RNPs encoding a luciferase reporter gene [59] using either all four PR8 RNP

373 polypeptides, or, to recapitulate RNPs of the 5:3 reassortant virus, PB1 from Cal7 and

374 PB2, PA and NP from PR8. In the latter “5:3” background, the PB2 and NP

375 polymorphisms were tested, singly and in combination, while a negative control lacked a

376 source of PB2. In all cases, increased transcriptional activity of the reconstituted RNPs

377 was observed at the cooler temperature of 35°C, while RNPs containing the Cal7 PB1

378 protein displayed greater transcriptional activity at both 35°C and 37.5°C than those

379 containing PR8 PB1 (Figure 5A). However, when the ratios of activities at 35°C:37.5°C

380 were calculated, the Cal7 PB1 did not confer greater temperature-dependency on the RNP

381 than the PR8 polypeptide (Figure 5A, green data points). Introducing the PB2 N701D and

382 NP T130A mutations into RNPs incubated at 37.5°C had relatively little effect on viral

383 gene expression, even when both changes were made to reconstitute X179A RNPs.

384 Surprisingly, the PB2 mutation significantly affected RNP activity at 35°C, but by

385 lowering it. Consequently, the ratios of activities at 35°C:37.5°C showed a clear effect of

386 the PB2 (but not the NP) mutation on the temperature-dependency of the RNP.

387 Examination of cell lysates by SDS-PAGE and western blotting for viral proteins PB2

388 and NP did not show any major differences in their accumulation (Figure 5B). Thus, in

389 the context of a ‘minireplicon’ assay, the Cal7 PB1 did not render RNPs more

Results

390 temperature sensitive, but the PR8 PB2 N701D polymorphism significantly affected the
391 temperature-dependency of the 5:3 virus RNP.

Results

392 **PB2 N701D reduces temperature sensitivity of the RG 5:3 virus**

393

394 To test the significance of the sequence polymorphisms between X-179A and our
395 PR8 internal genes, we attempted rescues of a panel of PR8:Cal7 5:3 viruses using either
396 the WT RG PR8 backbone, PB2 N701D, NP T130A, the NS mutant (NS1 K55E, M104I,
397 G113A, D120G and A132T, and NS2 E26G) or a ‘triple mutant’ containing the mutated
398 PB2, NP and NS genes that would, in protein-coding terms, recreate an RG X-179A.
399 Unexpectedly, viruses with the mutated segment 8 (either singly or as the triple mutant)
400 did not rescue on multiple attempts (data not shown). The reasons for this are not clear,
401 but are suggestive of a detrimental effect on virus replication. However, the PB2 and NP
402 mutants rescued readily and their growth in eggs was further characterised. When HA
403 yield of these viruses at 37.5°C and 35°C was assessed by HA assay, as before the 5:3WT
404 virus was temperature sensitive, giving significantly lower titres at 37.5°C (Figure 6A).
405 The NP mutant behaved similarly to WT at both temperatures, also showing strong
406 temperature sensitivity. In contrast, the PB2 N701D mutant showed a lesser (but still
407 statistically significant) drop in titre at 37.5°C and furthermore, gave significantly higher
408 HA titres than WT at both temperatures. To further test whether the PB2 N701D mutation
409 increased HA yield of the 5:3 CVV mimic, WT and PB2 mutant viruses were partially
410 purified from allantoic fluid and HA content examined by staining with Coomassie blue,
411 with or without prior de-glycosylation. Consistent with the HA titre data, both viruses
412 gave greater amounts of the major structural polypeptides NP, M1 and (best visualised
413 after de-glycosylation), HA following growth at 35°C than 37.5°C, with the PB2 mutant
414 out-performing the WT virus (Figure 6B, upper panel). Levels of de-glycosylated HA₁
415 were quantified by densitometry of western blots (Figure 6B, lower panel). Across three
416 replicate experiments, the 5:3WT virus gave on average a 3-fold increase in HA₁ yield at

Results

417 35C compared with 37.5°C, whereas the 5:3 PB2 N701D virus showed only a 1.7-fold
418 increase, confirming that the PB2 N701D polymorphism reduced the temperature
419 sensitivity of HA yield in eggs. Finally, we investigated the effects of temperature and the
420 PB2 mutation on the infectivity of the 5:3 viruses. As a measure of virus particle
421 infectivity, we derived genome copy to infectivity ratios for the WT 5:3 reassortant, the
422 PB2 mutant and the authentic X-179A HGR viruses grown at high and low temperatures.
423 RNA from virus pellets was extracted, reverse transcribed and quantitative real-time PCR
424 performed to determine the relative amounts of genome in virions. All viruses
425 incorporated similar levels of segments 2, 4, 5, 6 and 7 and there was no indication of
426 selective defective packaging of a particular segment from any of the viruses grown at the
427 different temperatures (data not shown). Virus infectivity was then determined for each
428 virus sample by TCID₅₀ assay and used to calculate genome copy:infectivity ratios,
429 normalised to the virus grown at 35°C. All viruses, including X-179A, showed worse
430 particle:infectivity ratios when grown at 37.5°C (Figure 6C). However, the WT 5:3 RG
431 reassortant virus had an approximately 250-fold higher genome:infectivity ratio than X-
432 179A when grown at 35°C and this was partially (but not completely) restored by the PB2
433 N701D change. Therefore, having PB2 701D is beneficial to the growth and HA yield of
434 a 5:3 CVV with pdm09 HA, NA and PB1.
435

Discussion

436 Discussion

437 Several studies in recent years have shown positive effects of incorporating WT
438 segment 2 into RG CVV mimics on yield for human pdm09 and H3N2 strains and avian
439 H5N1 and H7N9 strains [14-22]. In our study, we surprisingly found that for two pdm09
440 strains, an RG 6:2 virus containing the PR8 segment 2 gave higher HA yield in eggs than
441 the counterpart viruses containing the WT segment 2. Moreover, the RG 5:3 virus had a
442 markedly greater temperature sensitive phenotype compared with the RG 6:2 viruses, as
443 well as with very similar 5:3 genotype classical HGRs. Comparison of amino acid
444 sequence differences between our RG 5:3 viruses and authentic 5:3 HGRs suggested the
445 hypothesis that this was down to epistatic interactions between the WT segment 2 and
446 the internal PR8 genes. Further mutational analysis of the PR8 backbone employed here
447 indicated that the PB2 D701N polymorphism was a major contributor to this genetic
448 incompatibility.

449 Altering the backbone of our PR8 strain to contain PB2 701D did not completely
450 convert the phenotype of our RG 5:3 CVV mimic to that of its closest authentic HGR
451 counterpart, X-179A in terms of growth in eggs (Figure 6C). It may be that one or more
452 of the other amino acid polymorphisms between the PR8 genes in segments 5 and 8 also
453 contribute. The single difference in NP, T130A, did not affect minireplicon activity
454 (Figure 5) or HA yield in eggs (Figure 6 and data not shown). It lies in the RNA and PB2
455 binding regions of the protein but the functional significance of differences at this
456 residue are unclear. We were unable to test the significance of the segment 8
457 polymorphisms as the version of the segment mutated to match that in X-179A could not
458 be rescued into a viable virus, either singly, or when combined with the mutated segment
459 2 and 5 to supposedly recreate X-179A. The reasons for this are not clear. Possibly by
460 focussing on coding changes only, we missed an essential contribution from a non-

Discussion

461 coding change (of which there are several between our 5:3 Cal7 reassortant and X-179A,
462 not just in segment 8). Murakami *et al.*, 2008 showed that K55E (in the RNA binding
463 domain) of NS1 mediates growth enhancement of CVVs in MDCK cells [62]. The other
464 amino acid differences are in the effector domain of NS1: position 104 is adjacent to
465 residues known to affect interactions with the cellular cleavage and polyadenylation
466 specificity factor (CPSF), position 113 is in eukaryotic initiation factor 4GI (eIF4GI)
467 binding domain, position 120 is in the 123-127 PKR binding and potential polymerase
468 binding region and position 132 is close to a nuclear export signal (reviewed in [63]).
469 However, any effects of these precise amino acid differences in NS1 and NS2 are not
470 well documented.

471 The exact mechanism of how PB2 N701D reduces temperature sensitivity of our
472 RG-derived 5:3 virus remains to be elucidated, although our results suggest it may be at
473 the level of viral polymerase activity. Introducing this change into the PR8/Cal7 PB1
474 polymerase reduced the apparent temperature sensitivity of the viral RNP but by
475 decreasing activity at the lower temperature of 35 °C rather than by increasing activity at
476 the higher temperature (Figure 5). This does not permit a simple correlation to be drawn
477 between the effect of the mutation in the artificial sub-viral minireplicon assay and the
478 behaviour of the complete virus in eggs, but is nonetheless suggestive of a functionally
479 important link. The opposite change, PB2 D701N, has been shown to enhance the
480 interaction of PB2 with mammalian importin α 1 [52], so it would be interesting to
481 examine this from the perspective of adaptation to an avian host. Interactions between
482 PB2 and importin α have also been suggested to play a role in viral genome replication
483 [64]; the minireplicon assay used here primarily interrogates transcription, so this could
484 also be an avenue to explore further.

Discussion

485 Of the over a hundred PB2 sequences from conventionally reassorted viruses
486 (mostly X-series viruses) available on the Influenza Research Database (accessed
487 December 2018), the vast majority (117/118) have PB2 701D, with a single virus
488 having a glutamate residue. Of the 35 PR8 PB2 sequences available, 701N is a
489 minority variant, only appearing in two viruses; the one used here, and in a “high
490 growth” PR8 derived by serial passage in MDCK cells with the aim of producing a
491 high-yielding backbone constellation for RG vaccine reassortant production in
492 mammalian cells [65]. In this study, the parental PR8 virus possessed PB2 701D
493 before passaging and analysis of reassortant characteristics suggested that this
494 adaptive change was important for growth in cells. Moreover, it has been shown that
495 viruses with PB2 701N were detected in eggs incubated at 33°C but not at 37°C after
496 inoculation with a clinical specimen, suggesting that a lower temperature may be
497 favoured by PB2 701N viruses [66], similar to our study which shows that PB2 701N
498 has a temperature sensitive phenotype. The PR8 clone we used is a descendant of the
499 NIBSC PR8 strain used to make vaccine reassortants, produced by serial passage in
500 MDCK cells [39]; adaptive changes were not determined, but comparison with the
501 NIBSC PR8 PB2 sequence (data not shown) suggests that it did indeed acquire the
502 PB2 D701N change. The data reported here are the reciprocal of those reported by
503 Suzuki and colleagues [65] and further underscore the importance of PB2 701 as a
504 key residue for design of an optimal RG backbone depending on whether the
505 vaccine is to be grown in eggs or mammalian cells.

506

507 Acknowledgements

508

509 We thank Dr. Francesco Gubinelli, Dr. Carolyn Nicolson and Dr. Ruth Harvey at the
510 Influenza Resource Centre, National Institute for Biological Standards and Control,

Discussion

511 U. K. for their support during experiments performed in their lab. We also thank Dr.
512 Helen Wise from the Roslin Institute for useful discussions.

513

514 **Funding information**

515

516 This work was funded in part with Federal funds from the U.S. Department of Health
517 and Human Services, Office of the Assistant Secretary for Preparedness and
518 Response, Biomedical Advanced Research and Development Authority, under
519 Contract No. HHSO100201300005C (to OGE and PD), by a grant from UK
520 Department of Health's Policy Research Programme (NIBSC Regulatory Science
521 Research Unit), Grant Number 044/0069 (to OGE) as well as Institute Strategic
522 Programme Grants (BB/J01446X/1 and BB/P013740/1) from the Biotechnology and
523 Biological Sciences Research Council (BBSRC) to PD. The views expressed in the
524 publication are those of the author(s) and not necessarily those of the NHS, the
525 Department of Health, 'arms' length bodies or other government departments.

526 SH, MT, RMP and PD declare they have no conflict of interest. OGE and
527 JWMcC have received funding from the International Federation of Pharmaceutical
528 Manufacturers and Associations for the production of influenza candidate vaccine
529 viruses in eggs.

530

References

References

1. **WHO**. 2018. Influenza (Seasonal) Fact sheet [https://www.who.int/en/news-room/fact-sheets/detail/influenza-\(seasonal\)](https://www.who.int/en/news-room/fact-sheets/detail/influenza-(seasonal)) [accessed November 2018].
2. **Ito T, Suzuki Y, Takada A, Kawamoto A, Otsuki K et al**. Differences in sialic acid-galactose linkages in the chicken egg amnion and allantois influence human influenza virus receptor specificity and variant selection. *J Virol* 1997;71(4):3357-3362.
3. **Parker L, Wharton SA, Martin SR, Cross K, Lin Y et al**. Effects of egg-adaptation on receptor-binding and antigenic properties of recent influenza A (H3N2) vaccine viruses. *J Gen Virol* 2016;97(6):1333-1344.
4. **Raymond DD, Stewart SM, Lee J, Ferdman J, Bajic G et al**. Influenza immunization elicits antibodies specific for an egg-adapted vaccine strain. *Nat Med* 2016;22(12):1465-1469.
5. **Robertson JS, Bootman JS, Newman R, Oxford JS, Daniels RS et al**. Structural changes in the haemagglutinin which accompany egg adaptation of an influenza A(H1N1) virus. *Virology* 1987;160(1):31-37.
6. **Xu Q, Wang W, Cheng X, Zengel J, Jin H**. Influenza H1N1 A/Solomon Island/3/06 virus receptor binding specificity correlates with virus pathogenicity, antigenicity, and immunogenicity in ferrets. *J Virol* 2010;84(10):4936-4945.
7. **Zost SJ, Parkhouse K, Gumina ME, Kim K, Diaz Perez S et al**. Contemporary H3N2 influenza viruses have a glycosylation site that alters binding of antibodies elicited by egg-adapted vaccine strains. *Proc Natl Acad Sci U S A* 2017;114(47):12578-12583.
8. **Neumann G, Watanabe T, Ito H, Watanabe S, Goto H et al**. Generation of influenza A viruses entirely from cloned cDNAs. *Proc Natl Acad Sci U S A* 1999;96(16):9345-9350.
9. **Hoffmann E, Neumann G, Kawaoka Y, Hobom G, Webster RG**. A DNA transfection system for generation of influenza A virus from eight plasmids. *Proc Natl Acad Sci U S A* 2000;97(11):6108-6113.
10. **Fodor E, Devenish L, Engelhardt OG, Palese P, Brownlee GG et al**. Rescue of influenza A virus from recombinant DNA. *J Virol* 1999;73(11):9679-9682.
11. **Fulvini AA, Ramanunnair M, Le J, Pokorny BA, Arroyo JM et al**. Gene constellation of influenza A virus reassortants with high growth phenotype prepared as seed candidates for vaccine production. *PLoS One* 2011;6(6):e20823.
12. **Ramanunnair M, Le J, Onodera S, Fulvini AA, Pokorny BA et al**. Molecular signature of high yield (growth) influenza A virus reassortants prepared as candidate vaccine seeds. *PLoS One* 2013;8(6):e65955.
13. **Rudneva IA, Timofeeva TA, Shilov AA, Kochergin-Nikitsky KS, Varich NL et al**. Effect of gene constellation and postreassortment amino acid change on the phenotypic features of H5 influenza virus reassortants. *Arch Virol* 2007;152(6):1139-1145.
14. **Plant EP, Ye Z**. Chimeric neuraminidase and mutant PB1 gene constellation improves growth and yield of H5N1 vaccine candidate virus. *J Gen Virol* 2015;96(Pt 4):752-755.
15. **Plant EP, Liu TM, Xie H, Ye Z**. Mutations to A/Puerto Rico/8/34 PB1 gene improves seasonal reassortant influenza A virus growth kinetics. *Vaccine* 2012;31(1):207-212.

References

16. **Cobbin JC, Verity EE, Gilbertson BP, Rockman SP, Brown LE.** The source of the PB1 gene in influenza vaccine reassortants selectively alters the hemagglutinin content of the resulting seed virus. *J Virol* 2013;87(10):5577-5585.
17. **Cobbin JC, Ong C, Verity E, Gilbertson BP, Rockman SP et al.** Influenza virus PB1 and neuraminidase gene segments can cosegregate during vaccine reassortment driven by interactions in the PB1 coding region. *J Virol* 2014;88(16):8971-8980.
18. **Wanitchang A, Kramyu J, Jongkaewwattana A.** Enhancement of reverse genetics-derived swine-origin H1N1 influenza virus seed vaccine growth by inclusion of indigenous polymerase PB1 protein. *Virus Res* 2010;147(1):145-148.
19. **Gomila RC, Suphaphiphat P, Judge C, Spencer T, Ferrari A et al.** Improving influenza virus backbones by including terminal regions of MDCK-adapted strains on hemagglutinin and neuraminidase gene segments. *Vaccine* 2013;31(42):4736-4743.
20. **Giria M, Santos L, Louro J, Rebelo de Andrade H.** Reverse genetics vaccine seeds for influenza: Proof of concept in the source of PB1 as a determinant factor in virus growth and antigen yield. *Virology* 2016;496:21-27.
21. **Mostafa A, Kanrai P, Ziebuhr J, Pleschka S.** The PB1 segment of an influenza A virus H1N1 2009pdm isolate enhances the replication efficiency of specific influenza vaccine strains in cell culture and embryonated eggs. *J Gen Virol* 2016;97(3):620-631.
22. **Gilbertson B, Zheng T, Gerber M, Printz-Schweigert A, Ong C et al.** Influenza NA and PB1 Gene Segments Interact during the Formation of Viral Progeny: Localization of the Binding Region within the PB1 Gene. *Viruses* 2016;8:238.
23. **Gog JR, Afonso Edos S, Dalton RM, Leclercq I, Tiley L et al.** Codon conservation in the influenza A virus genome defines RNA packaging signals. *Nucleic Acids Res* 2007;35(6):1897-1907.
24. **Hutchinson EC, von Kirchbach JC, Gog JR, Digard P.** Genome packaging in influenza A virus. *J Gen Virol* 2010;91(Pt 2):313-328.
25. **Barman S, Krylov PS, Turner JC, Franks J, Webster RG et al.** Manipulation of neuraminidase packaging signals and hemagglutinin residues improves the growth of A/Anhui/1/2013 (H7N9) influenza vaccine virus yield in eggs. *Vaccine* 2017;35:1424-1430.
26. **Adamo JE, Liu T, Schmeisser F, Ye Z.** Optimizing viral protein yield of influenza virus strain A/Vietnam/1203/2004 by modification of the neuraminidase gene. *J Virol* 2009;83(9):4023-4029.
27. **Pan W, Dong Z, Meng W, Zhang W, Li T et al.** Improvement of influenza vaccine strain A/Vietnam/1194/2004 (H5N1) growth with the neuraminidase packaging sequence from A/Puerto Rico/8/34. *Hum Vaccin Immunother* 2012;8(2):252-259.
28. **Jing X, Phy K, Li X, Ye Z.** Increased hemagglutinin content in a reassortant 2009 pandemic H1N1 influenza virus with chimeric neuraminidase containing donor A/Puerto Rico/8/34 virus transmembrane and stalk domains. *Vaccine* 2012;30(28):4144-4152.
29. **Harvey R, Nicolson C, Johnson RE, Guilfoyle KA, Major DL et al.** Improved haemagglutinin antigen content in H5N1 candidate vaccine viruses with chimeric haemagglutinin molecules. *Vaccine* 2010;28(50):8008-8014.
30. **Harvey R, Johnson RE, MacLellan-Gibson K, Robertson JS, Engelhardt OG.** A promoter mutation in the haemagglutinin segment of influenza A virus

References

- generates an effective candidate live attenuated vaccine. *Influenza Other Respir Viruses* 2014;8(6):605-612.
31. **Harvey R, Guilfoyle KA, Roseby S, Robertson JS, Engelhardt OG.** Improved antigen yield in pandemic H1N1 (2009) candidate vaccine viruses with chimeric hemagglutinin molecules. *J Virol* 2011;85(12):6086-6090.
 32. **Medina J, Boukhebz H, De Saint Jean A, Sodoyer R, Legastelois I et al.** Optimization of influenza A vaccine virus by reverse genetic using chimeric HA and NA genes with an extended PR8 backbone. *Vaccine* 2015;33(35):4221-4227.
 33. **Chen W, Calvo PA, Malide D, Gibbs J, Schubert U et al.** A novel influenza A virus mitochondrial protein that induces cell death. *Nat Med* 2001;7(12):1306-1312.
 34. **Fodor E.** The RNA polymerase of influenza a virus: mechanisms of viral transcription and replication. *Acta Virol* 2013;57(2):113-122.
 35. **Wise HM, Foeglein A, Sun J, Dalton RM, Patel S et al.** A complicated message: Identification of a novel PB1-related protein translated from influenza A virus segment 2 mRNA. *J Virol* 2009;83(16):8021-8031.
 36. **Johnson A, Chen LM, Winne E, Santana W, Metcalfe MG et al.** Identification of Influenza A/PR/8/34 Donor Viruses Imparting High Hemagglutinin Yields to Candidate Vaccine Viruses in Eggs. *PLoS One* 2015;10(6):e0128982.
 37. **Matrosovich M, Matrosovich T, Carr J, Roberts NA, Klenk HD.** Overexpression of the alpha-2,6-sialyltransferase in MDCK cells increases influenza virus sensitivity to neuraminidase inhibitors. *J Virol* 2003;77(15):8418-8425.
 38. **Moscovici C, Moscovici MG, Jimenez H, Lai MM, Hayman MJ et al.** Continuous tissue culture cell lines derived from chemically induced tumors of Japanese quail. *Cell* 1977;11(1):95-103.
 39. **de Wit E, Spronken MI, Bestebroer TM, Rimmelzwaan GF, Osterhaus AD et al.** Efficient generation and growth of influenza virus A/PR/8/34 from eight cDNA fragments. *Virus Res* 2004;103(1-2):155-161.
 40. **Elderfield RA, Watson SJ, Godlee A, Adamson WE, Thompson CI et al.** Accumulation of human-adapting mutations during circulation of A(H1N1)pdm09 influenza virus in humans in the United Kingdom. *J Virol* 2014;88(22):13269-13283.
 41. **Turnbull ML, Wise HM, Nicol MQ, Smith N, Dunfee RL et al.** Role of the B Allele of Influenza A Virus Segment 8 in Setting Mammalian Host Range and Pathogenicity. *J Virol* 2016;90(20):9263-9284.
 42. **Zhang Y, Aevermann BD, Anderson TK, Burke DF, Dauphin G et al.** Influenza Research Database: An integrated bioinformatics resource for influenza virus research. *Nucleic Acids Res* 2017;45(D1):D466-D474.
 43. **Noton SL, Medcalf E, Fisher D, Mullin AE, Elton D et al.** Identification of the domains of the influenza A virus M1 matrix protein required for NP binding, oligomerization and incorporation into virions. *J Gen Virol* 2007;88(Pt 8):2280-2290.
 44. **Amorim MJ, Read EK, Dalton RM, Medcalf L, Digard P.** Nuclear export of influenza A virus mRNAs requires ongoing RNA polymerase II activity. *Traffic* 2007;8(1):1-11.
 45. **Mullin AE, Dalton RM, Amorim MJ, Elton D, Digard P.** Increased amounts of the influenza virus nucleoprotein do not promote higher levels of viral genome replication. *J Gen Virol* 2004;85(Pt 12):3689-3698.
 46. **Klimov A, Balish A, Veguilla V, Sun H, Schiffer J et al.** Influenza virus titration, antigenic characterization, and serological methods for antibody detection. *Methods Mol Biol* 2012;865:25-51.

References

47. **CDC**. 2009. CDC protocol of realtime RTPCR for influenza A(H1N1) https://www.who.int/csr/resources/publications/swineflu/CDCRealtimeRTPCR_SwineH1Assay-2009_20090430.pdf [accessed October 2016].
48. **Benfield CT, Lyall JW, Kochs G, Tiley LS**. Asparagine 631 variants of the chicken Mx protein do not inhibit influenza virus replication in primary chicken embryo fibroblasts or in vitro surrogate assays. *J Virol* 2008;82(15):7533-7539.
49. **Dobbelaer R, Levandowski, R., Wood, J**. Recommendations for production and control of influenza vaccine (inactivated). WHO technical series. 2003.
50. **Brown EG, Liu H, Kit LC, Baird S, Nesrallah M**. Pattern of mutation in the genome of influenza A virus on adaptation to increased virulence in the mouse lung: identification of functional themes. *Proc Natl Acad Sci U S A* 2001;98(12):6883-6888.
51. **Gabriel G, Dauber B, Wolff T, Planz O, Klenk HD et al**. The viral polymerase mediates adaptation of an avian influenza virus to a mammalian host. *Proc Natl Acad Sci U S A* 2005;102(51):18590-18595.
52. **Gabriel G, Herwig A, Klenk HD**. Interaction of polymerase subunit PB2 and NP with importin alpha1 is a determinant of host range of influenza A virus. *PLoS Pathog* 2008;4(2):e11.
53. **Gabriel G, Klingel K, Otte A, Thiele S, Hudjetz B et al**. Differential use of importin-alpha isoforms governs cell tropism and host adaptation of influenza virus. *Nat Commun* 2011;2:156.
54. **Gao Y, Zhang Y, Shinya K, Deng G, Jiang Y et al**. Identification of amino acids in HA and PB2 critical for the transmission of H5N1 avian influenza viruses in a mammalian host. *PLoS Pathog* 2009;5(12):e1000709.
55. **Li Z, Chen H, Jiao P, Deng G, Tian G et al**. Molecular basis of replication of duck H5N1 influenza viruses in a mammalian mouse model. *J Virol* 2005;79(18):12058-12064.
56. **Ping J, Dankar SK, Forbes NE, Keleta L, Zhou Y et al**. PB2 and Hemagglutinin Mutations Are Major Determinants of Host Range and Virulence in Mouse-Adapted Influenza A Virus. *Journal of Virology* 2010;84(20):10606-10618.
57. **Steel J, Lowen AC, Mubareka S, Palese P**. Transmission of influenza virus in a mammalian host is increased by PB2 amino acids 627K or 627E/701N. *PLoS Pathog* 2009;5(1):e1000252.
58. **Zhou B, Pearce MB, Li Y, Wang J, Mason RJ et al**. Asparagine substitution at PB2 residue 701 enhances the replication, pathogenicity, and transmission of the 2009 pandemic H1N1 influenza A virus. *PLoS One* 2013;8(6):e67616.
59. **Foeglein A, Loucaides EM, Mura M, Wise HM, Barclay WS et al**. Influence of PB2 host-range determinants on the intranuclear mobility of the influenza A virus polymerase. *Journal of General Virology* 2011;92(7):1650-1661.
60. **Labadie K, Dos Santos Afonso E, Rameix-Welti MA, van der Werf S, Naffakh N**. Host-range determinants on the PB2 protein of influenza A viruses control the interaction between the viral polymerase and nucleoprotein in human cells. *Virology* 2007;362(2):271-282.
61. **Massin P, van der Werf S, Naffakh N**. Residue 627 of PB2 is a determinant of cold sensitivity in RNA replication of avian influenza viruses. *J Virol* 2001;75(11):5398-5404.
62. **Murakami S, Horimoto T, Mai le Q, Nidom CA, Chen H et al**. Growth determinants for H5N1 influenza vaccine seed viruses in MDCK cells. *J Virol* 2008;82(21):10502-10509.

References

63. **Hale BG, Randall RE, Ortin J, Jackson D.** The multifunctional NS1 protein of influenza A viruses. *J Gen Virol* 2008;89(Pt 10):2359-2376.
64. **Resa-Infante P, Jorba N, Zamarreno N, Fernandez Y, Juarez S et al.** The host-dependent interaction of alpha-importins with influenza PB2 polymerase subunit is required for virus RNA replication. *PLoS One* 2008;3(12):e3904.
65. **Suzuki Y, Odagiri T, Tashiro M, Nobusawa E.** Development of an Influenza A Master Virus for Generating High-Growth Reassortants for A/Anhui/1/2013(H7N9) Vaccine Production in Qualified MDCK Cells. *PLoS One* 2016;11(7):e0160040.
66. **Le QM, Sakai-Tagawa Y, Ozawa M, Ito M, Kawaoka Y.** Selection of H5N1 influenza virus PB2 during replication in humans. *J Virol* 2009;83(10):5278-5281.

Figures and tables

TABLE 1. Taqman primers and probes for amplification of Influenza genomic segments by real time RT-PCR

Segment	Strain	Forward primer 5'-3'	Reverse primer 5'-3'	Probe 5' FAM- 3' TAMRA	Nucleotide position of amplicon
2	Cal7	GCTCCAATCATCCGACGATT	CTGCTTGTATTCCCTCATGGTTT	CTCTCATAGTGAATGCAC	1344-1408
4'	Cal7	GTGCTATAAACACCAGCTCCCA	CGGGATATTCTCAATCCTGTGGC	CAGAATATACATCCGATACAATTGGAAAA	934-1049
6	Cal7	AATCACATGTGTGTGCAGGGATA	GAAAGACACCCACGGTCGAT	CTGGCATGGCTCG	881-938
2	PR8	GAGATACACCAAGACTACTTA	GGTGCATTACAATCAGAG	CTGGTGGGATGGTCTTCAATCCTC	1311-1385
5	PR8	AGCATTC AATGGGAATACAGA	CCCTGGAAAGACACATCTT	TCTGACATGAGGACCGAAATCATAAGGA	1326-1424
7	PR8	CCTGGTATGTGCAACCTGTGAA	TGGATTGGTTGTTGTCACCATT	AGATTGCTGACTCCCAGCATCGG	460-538

*Primer/probe sequences for Cal7 segment 4 obtained from the CDC [47].

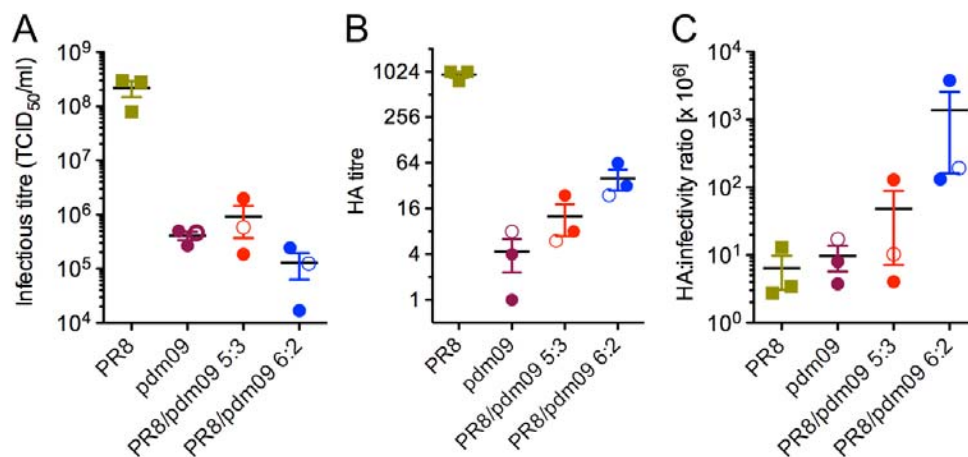


FIGURE 1. Effect of segment 2 source on virus growth. Virus stocks were grown in eggs and titred by **A)** TCID₅₀ assay on MDCK-SIAT cells or **B)** by HA assay. **C)** shows the ratio of HA: infectivity titres, arbitrarily scaled by a factor of 10⁶. Data points are from independently rescued stocks. Filled circles represent viruses with Cal7 glycoproteins and open circles Eng195. Bars represent the mean and SEM.

Figures and tables

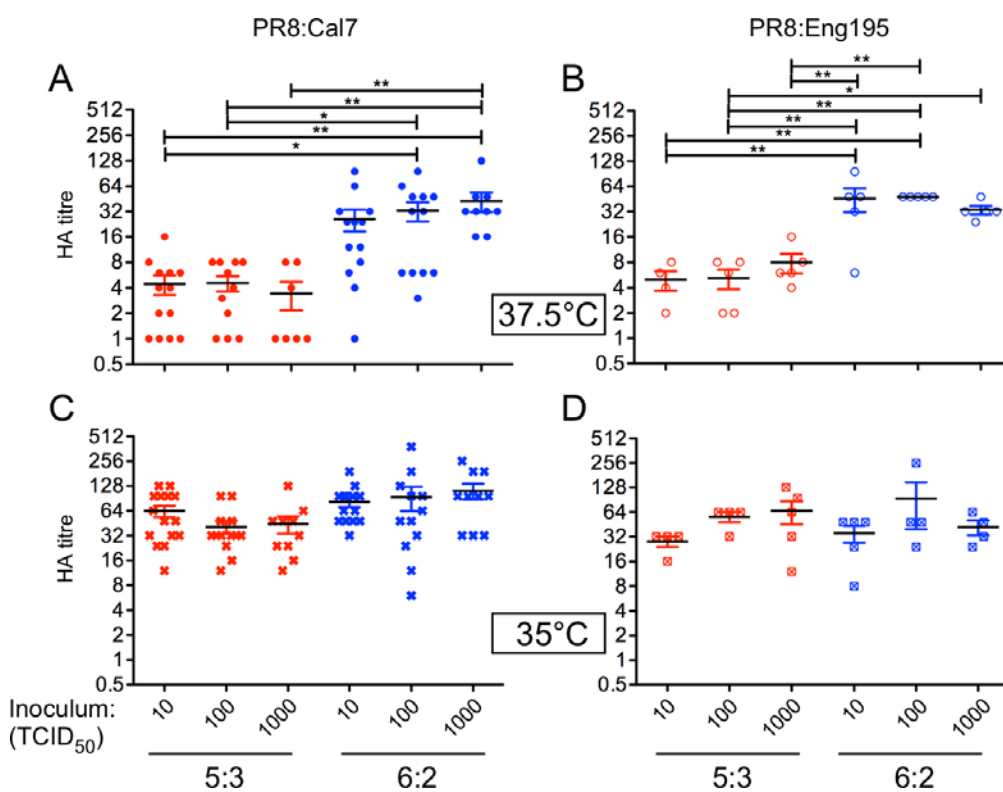


FIGURE 2. HA yield of PR8:pdm09 5:3 and 6:2 CVV mimics grown at 37.5°C or 35°C. HA titres from allantoic fluid of embryonated eggs infected with reassortants derived from **A, C**) Cal7 or **B, D**) Eng195 grown at 37.5°C (**A, B**) or 35°C (**C, D**) at 3 days p.i. Bars indicate mean and SEM of 3 independent experiments (5 eggs per condition in an experiment) for PR8:Cal7 reassortants (from two independently rescued RG stocks), and a single experiment for PR8:Eng195 reassortants. Horizontal bars indicate statistical significance (*p < 0.05, **p < 0.01), assessed by Tukey's test.

Figures are tables

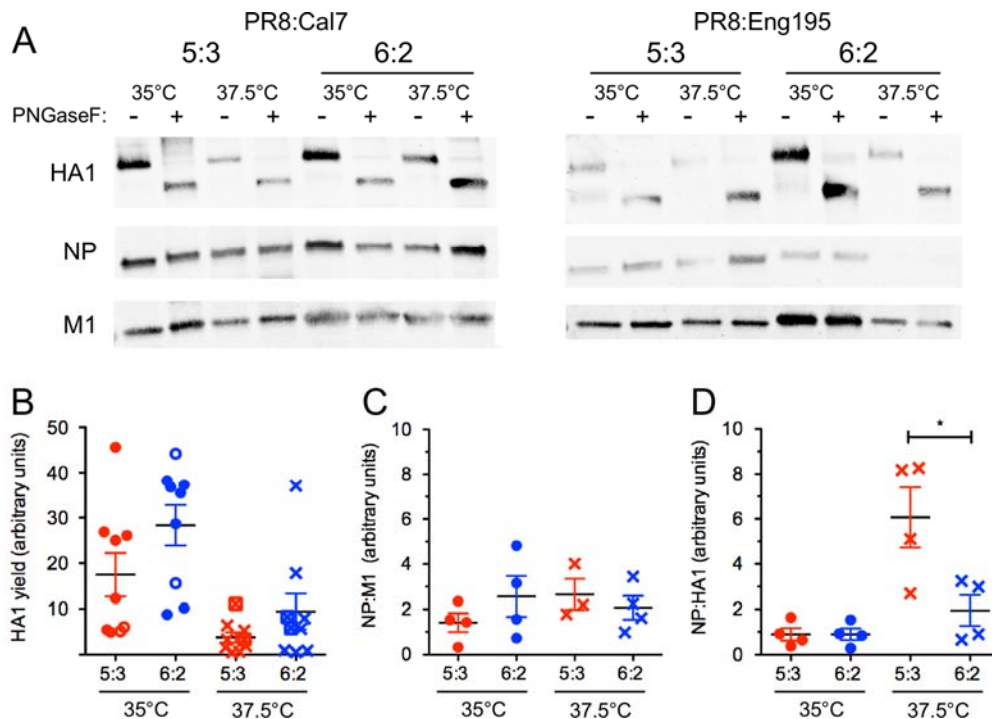


FIGURE 3. Relative virion composition of viruses grown at 37.5°C versus 35°C. Western blots of purified virus preparations from allantoic fluid of embryonated eggs infected with **A**) PR8:Cal7 or **B**) PR8:Eng195 reassortants grown at 37.5°C or 35°C at 3 days p.i. Equal volumes of virus samples were either treated with PNGase F (+) or left untreated (-), separated by SDS-PAGE on a 4-20% polyacrylamide gel and virus proteins HA₁, NP and M1 detected by western blotting and quantified by densitometry. **C, D, E**) Ratios of NP:HA₁ (de-glycosylated), NP:M1 and M1:HA₁ (de-glycosylated) respectively. Bars indicate mean and SEM from 5 independent virus yield experiments (4 experiments with PR8:Cal7 reassortants (filled symbols) using 2 independent RG stocks and a single experiment with PR8:Eng195 reassortants (open symbols)). Horizontal bars indicate statistical significance assessed by Tukey's test (*p < 0.05).

Figures and tables

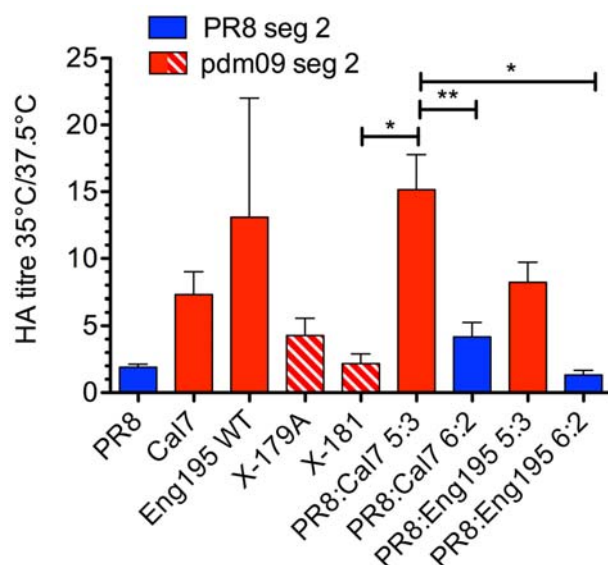


FIGURE 4. Relative HA titre of RG WT, RG reassortant and HGR viruses containing pdm09 or PR8 segment 2 at 35 °C versus 37.5 °C. For each independent experiment, the fold increase in HA titre of viruses grown at 35°C versus 37.5°C at 3 days p.i. was calculated. Bars indicate mean and SEM from 2-10 independent experiments for each virus. Horizontal bars indicate statistical significance (* $p < 0.05$, ** $p < 0.01$), assessed by Tukey's test.

Figures and tables

Table 2. Amino acid sequence differences between RG CVV mimic and HGR viruses

A)

Protein	Cal7	Eng195	X-179A	X-181
PB1		K353R		
HA	T209K	L32I, P83S, T209K, R223Q, I321V		N129D
NA				

B)

Protein	No. differences PR8 vs X-179A	Amino acid changes (PR8 > X-179A)
PB2	1	N701D
PA	0	
NP	1	T130A
M1 (M2)	0	
NS1 (NS2)	5 (1)	K55E, M104I, G113A, D120G, A132T (E26G)

A). Variations from the consensus sequences of the pdm09 PB1, HA and NA polypeptides of the indicated viruses. Sequence accession numbers (segments 2,4 and 6 respectively): Cal7 EPI1355048, EPI1355049, EPI1355051; Eng195 GQ166655.1, GQ166661.1, GQ166659.1; X-179-A CY058517.1, CY058519, CY058521; X-181 GQ906800, GQ906801, GQ906802.

B). Sequence differences between the backbone-encoded polypeptides of RG PR8 and X-179A. Sequence accession numbers (segments 1,3, 5, 7, 8 respectively): PR8 EF467818, EF467820, EF467822, EF467824, EF467817; X179A CY058516, CY058518, CY058520, CY058522, CY058523.

Figures and tables

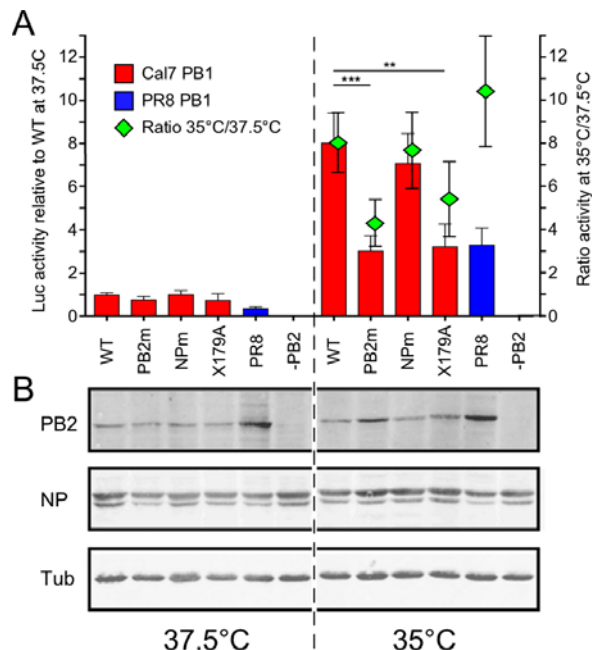
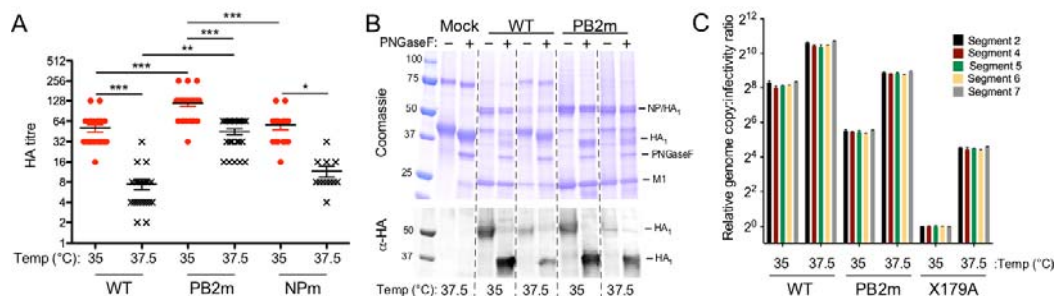


FIGURE 5. Effect of temperature on RNP activity in avian cells. QT-35 cells were co-transfected with plasmids expressing a synthetic vRNA encoding luciferase along with either Cal7 (red bars) or PR8 PB1 (blue bars) as well as PA, PB2 and NP from PR8, with PB2 and NP either being WT or PB2 N701D (PB2m) and/or NP T130A (NPm) as indicated (RNPs reconstituted with the Cal7 PB1 and both PB2 and NP mutants are equivalent to and labelled as X-179A). Replicate transfections were incubated at 37.5°C or 35°C and at 48 h post-transfection, cells were lysed and luciferase activity measured. **A)** Luciferase activity at each temperature was calculated as fold increases over a negative control lacking PB2 (-PB2), and then normalised to the activity seen from RNPs with Cal7 PB1 and WT PR8 PB2, PA and NP components (WT) at 37.5°C. Data are plotted as bar graphs using the left hand y axis. Statistical significance is indicated (** $p < 0.01$, *** $p < 0.001$), assessed by Tukey's test. To assess the temperature sensitivity of the various RNPs, the ratio of activity at 35°C:37.5°C was calculated and plotted as column means (green diamonds) using the right hand y axis. All values are mean and SEM of 4 independent experiments, with transfections performed in triplicate. **B)** Cell lysates from parallel transfections were analysed by SDS-PAGE and western blotting for viral proteins PB2 and NP. Tubulin (tub) was employed as a loading control.

Figures and tables



1
2
3
4
5
6
7
8
9
10
11
12
13
14
15
16
17
18
19
20
21

FIGURE 6. Yield assessment of PR8:Cal7 5:3 mutants grown in eggs at 35°C and 37.5°C. **A)** HA titres from allantoic fluid of embryonated eggs infected with PR8:Cal7 6:2 and 5:3 mutants grown in eggs at 35°C and 37.5°C at 3 days p.i. Bars indicate mean and SEM from 4 independent experiments using 2 independently rescued stocks of virus for WT and PB2m and 3 independent experiments with a single rescue for NPm (4 - 7 eggs per condition in an experiment). Statistical significance is indicated (* $p < 0.05$, ** $p < 0.01$, *** $p < 0.001$), assessed by Tukey's test. **B)** Representative SDS-PAGE of partially purified virus from pooled allantoic fluid. Equal volumes of each virus sample were either treated with PNGase F (+) or left untreated (-), separated by SDS-PAGE on a 4-20% polyacrylamide gel and analysed by (upper panel) Coomassie staining or (lower panel) western blotting to detect HA₁. Molecular mass markers (kDa) are also shown. **C)** RNA was extracted from virus pellets and qRT-PCR performed to quantify amounts of the indicated segments. Data are plotted as the ratio of genome copy number to infectivity (separately determined by TCID₅₀ assay) relative to the value obtained for X-179A grown at 35°C. Error bars reflect the mean and standard deviation of qPCR performed in triplicate per sample.